



Self-supported carbon veil biosensor architecture for voltammetric lactose determination in dairy products

Kamila Karaguzina ^a , Dmitry Stoikov ^{a*} , Elizaveta Silina ^a , Dominika Kappo ^a , Alexey Rogov ^a , Ivan Stoikov ^a

^a: Alexander Butlerov Institute of Chemistry, Kazan Federal University , Kazan 420008, Russia

* Corresponding author: DmIStojkov@kpfu.ru

Abstract

The global rise in the prevalence of lactose intolerance has increased the demand for sensitive analytical platforms to monitor low-lactose and lactose-free dairy products. This work details the development of a novel, standalone carbon veil electrode and its application in a cascade biosensing system. The electrode fabrication involves a simple, self-supported design where the carbon veil fibers are localized using a cyanoacrylate dielectric barrier, preventing capillary effects while maintaining a highly accessible 3D macroporous architecture. The carbon veil electrode surface was modified with a supramolecular nanocomposite of silver nanoparticles and pillar[5]arene, followed by the reagent-less immobilization of lactase. Pillar[5]arene facilitates the formation of stable silver nanoparticles and acts as an electron transfer mediator, enhancing the analytical signal through host-guest pre-concentration of the analyte. The biosensor utilizes a dual cascade mechanism: enzymatic hydrolysis of lactose generates glucose, which is then oxidized at the silver nanoparticles catalytic centers. The system exhibited a limit of detection of 3.2 nM and a linear range from 1×10^{-8} to 2×10^{-4} M. To mitigate matrix effects in complex dairy samples, a preparation protocol involving protein precipitation and centrifugation was developed. Practical performance was evaluated using milk and yogurt samples, employing a sequential measurement strategy and matrix-matched calibration to eliminate interference from endogenous glucose. The developed platform provides a robust, scalable, and cost-effective tool for food quality control and personalized nutrition monitoring.

Key findings

- A carbon veil-based enzyme biosensor was developed for highly sensitive and rapid lactose determination.
- The carbon veil electrode combined with pillar[5]arene-stabilized silver nanoparticles significantly enhances the analytical signal.
- The lactose concentration ranges from 10 nM to 20 mM with a detection limit of 3.2 nM.

© 2026, the Authors. This article is published in open access under the terms and conditions of the Creative Commons Attribution (CC BY) license (<http://creativecommons.org/licenses/by/4.0/>), which permits unrestricted reuse of the work in any medium provided the original work is properly cited.

1. Introduction

Electrochemical sensors are in high demand due to their low cost [1], rapid response [2], and high sensitivity [3]. A significant advantage of such devices is the potential for miniaturization, which enhances their portability [4]. Enzymatic biosensors, which convert biochemical interaction with an analyte into a measurable electrical signal [5].

Lactose, the primary disaccharide found in milk and dairy products, holds a special place among analyzed biochemical markers [6]. Monitoring lactose using lactase is critical for the food industry and clinical diagnostics [7] due to the global rise in lactose intolerance [8] and related gastrointestinal disorders [9], necessitating reliable tools for strict dietary control [10]. While traditional instrumental

Accompanying information

Article history

Received: 05.04.2026

Revised: 03.05.2026

Accepted: 04.05.2026

Available online: 04.05.2026

Keywords

Enzyme sensor; biosensor; lactose; nanoparticles; pillar[5]arene; carbon veil

Funding

The research was supported by the grant of the Russian Science Foundation № 25-73-10116, <https://rscf.ru/en/project/25-73-10116/>.

Supplementary information

Supplementary materials:

Transparent peer review:

Sustainable Development Goals



methods like chromatography [11], capillary electrophoresis [12], and spectroscopy [13] offer high accuracy, their complexity makes electrochemical biosensors a promising alternative for creating compact, user-friendly devices [14]. In this context, electrochemical biosensors represent a promising alternative.

However, modern biosensors face the challenge of enzyme immobilization: traditional polymer membranes create diffusion barriers and reduce catalytic activity [15]. Carbon nanomaterials serve as a promising solution to this architectural problem [16]. Previously, our group successfully demonstrated the effectiveness of a composite consisting of a macroporous carbon veil and the pillar[5]arene (P[5]A) macrocycle for creating cascade biosensors on solid-phase supports [17]. Carbon veil is a structural material with a non-woven structure made of smooth, long, cylindrical fibers forming a network with macro-sized gaps between the fibers, resulting in the high porosity of the veil [18]. Due to its unique structure, carbon veil is capable of increasing the effective surface area of the working electrode [19].

Due to its chemical and thermal stability [18], conductive properties, high specific surface area, and low cost, carbon veil can serve as an ideal material both as a working electrode modifier and as a platform for creating the electrodes and electrochemical systems themselves. There are reports in the literature regarding the development of electrodes based on non-woven carbon materials: a working electrode on a platform of carbon paper treated with a pulsed laser and modified with a nanoporous nickel network [20], working and auxiliary electrodes made of carbon paper on a screen-printed copy paper platform [21], a working electrode on a platform of carbon paper and aluminum foil [22], and others.

Devices of non-analytical purpose are primarily presented in the literature based on carbon veil electrodes: electrosynthetic biofilms for microbial electrosynthesis [23], microbial fuel cells [18], and electrochemical capacitors [24]. At the same time, sources [25-27] also present technologies for fabricating working electrodes from carbon veil and a polymer substrate, used both in unmodified form and in combination with various carbon materials and nanocomposite coatings, for the determination of a range of food dyes, uric acid, and ascorbic acid. However, these methods for creating carbon veil electrodes remain labor-intensive, requiring hot lamination onto substrates and the use of complex adhesive mixtures. In the present study, a simplified approach is proposed for the creation of an independent self-supported veil electrode (VE). The elimination of laminating substrates and the local impregnation of the fiber with cyanoacrylate glue (to prevent the capillary effect [28]) allowed for a multiple-fold reduction in assembly cost and time.

To ensure high sensitivity and accelerate electron transfer, the VE surface was modified with P[5]A. In the developed system, this macrocycle coordinates silver ions, reducing them to their metallic form [29] directly on the carbon

fibers. The resulting silver nanoparticles (AgNPs) served as powerful electrocatalytic centers. Sensors whose mechanism of action is based on the oxidation of glucose by metals and their compounds are among the common non-enzymatic methods for glucose determination [30].

A key feature of the developed platform is the advancement of the previously effective concept of cascade signal amplification [17] through the implementation of a dual cascade mechanism without the use of additional signal-blocking binder components. Within this cascade, lactose is enzymatically cleaved by lactase, and the resulting glucose undergoes instantaneous, highly sensitive non-enzymatic oxidation at the AgNPs.

Accordingly, in this work, we have proposed a VE modified with the P[5]A/AgNPs/lactase composite - an ultra-compact, scalable, and low-cost biosensor that represents an excellent candidate for implementation as a portable analytical device for rapid lactose monitoring with a nanomolar limit of detection in real food products and clinical practice.

2. Materials and methods

2.1. Reagents

HEPES, AgNO₃, glucose, lactase (β -Galactosidase) from *Escherichia coli* (500 units/mg protein) from Sigma-Aldrich (USA), carbon veil from Composite Polymer (Russia) were used. All other reagents were of chemical grade purity. The solutions were prepared using deionized water from a Millipore Q Simplicity® water purification system (Merck Millipore, France).

P[5]A (Fig. S1) was synthesized according to a previously reported method [31].

2.2. Development of the working VE

VE (Fig. 1) was prepared by cutting rectangles 3 mm in width, 0.4 mm in thickness, and of varying length from a carbon veil sheet. At the junction between the working part and the current collector, the fiber was impregnated with cyanoacrylate glue to form a protective sealant.

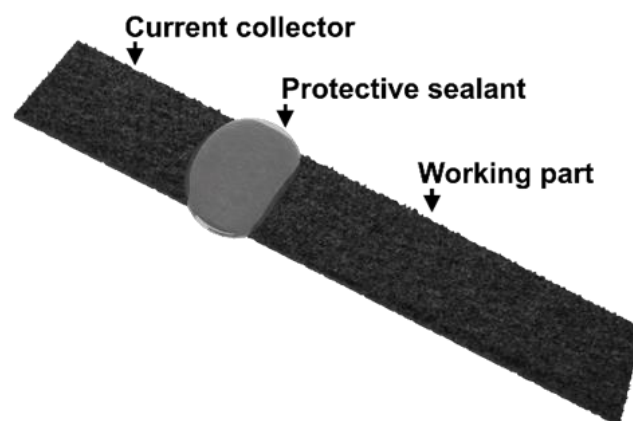


Figure 1 Scheme of the VE.

2.3. Modification of the VE surface with AgNPs and lactase

To prepare 100 μL of the AgNPs/P[5]A dispersion, 10 μL of 0.1 M AgNO_3 and 80 μL of 10 mM P[5]A were mixed and incubated for 30 minutes. Subsequently, the VE was modified by drop-casting 100 μL of the AgNPs/P[5]A dispersion. The AgNPs/P[5]A/VE was then modified by drop-casting an aliquot of lactase solution containing 2 units of enzymatic activity.

2.4. Voltammetric measurements

Cyclic voltammograms were recorded in the potential ranges from -0.5 to 0.7 V for the characterization of the VE electrochemical behavior, and from -0.5 to 0.5 V for the modified VE, at a scan rate of 0.1 V/s. Differential pulse voltammograms were recorded in the range from -0.4 to 0.4 V, with a potential step of 0.004 V, an amplitude of 0.05 V, a pulse width of 0.06 s, and a pulse interval of 0.5 s. All measurements were performed in a HEPES buffer solution containing 0.1 M NaNO_3 (pH 7.0). The voltammograms were recorded using a CHI 660E potentiostat (CH Instruments Inc., USA). The developed self-supported VE served as the working electrode. A platinum wire and an Ag/AgCl electrode were employed as the counter and reference electrodes, respectively.

2.5. Lactose determination in the dairy products samples

Dairy products (ultra-pasteurized milk and yogurt) samples were purchased from a local supermarket. To minimize working electrode surface passivation by the sample macromolecules, a specific sample preparation procedure was employed [32]. An aliquot of the thoroughly mixed sample (1 g) was transferred to a volumetric flask. Protein precipitation was performed by the sequential addition of 1 mL of ZnSO_4 and 1 mL of trichloroacetic acid under vigorous stirring. The solution was adjusted to pH 7.0 using 0.25 M NaOH, diluted to volume with distilled water, and incubated for 15 minutes at room temperature. To obtain a clear analyte, the mixture was centrifuged, and the resulting supernatant was further diluted with the supporting electrolyte (HEPES buffer with 0.1 M NaNO_3 , pH 7.0).

Lactose determination was carried out using differential pulse voltammetry. To account for matrix effects and ensure high accuracy, a matrix-matched calibration was constructed using one of the prepared supernatants. This procedure allowed for the effective evaluation of the biosensor's performance in a complex dairy matrix and the mitigation of interference from endogenous components. The analytical performance of the biosensor was evaluated by adding known concentrations of lactose to the buffer solution. Differential pulse voltammograms were recorded after each addition to establish the calibration dependence and determine the limit of detection (LOD).

2.6. Scanning Electron Microscopy

Scanning electron microscopy (SEM) images of the electrode coatings were obtained with the high-resolution field emission scanning electron microscope MerlinTM (CarlZeiss, Germany). The images were recorded in secondary electron (SE) mode. Due to the high electrical conductivity of the carbon veil, the samples were fixed on a conductive tape and imaged directly without any additional metal or carbon sputtering.

3. Results and discussion

The development of high-sensitivity electrochemical biosensors is inextricably linked to the search for electrode materials capable of overcoming the diffusion limitations of traditional planar platforms. In this context, carbon veil, which consists of a chaotic 3D network of intertwined smooth microfibers, serves as a promising matrix. Unlike classical solid-state electrodes (e.g., glassy carbon electrode or screen-printed electrodes on rigid substrates), the unique open 3D structure of carbon veil is accessible for substrate diffusion from all sides, which manifoldly increases the effective surface area of the working electrode.

3.1. VE: Fabrication method and electrochemical properties

VEs were fabricated by cutting rectangular fragments 3 mm in width and of varying lengths from a carbon veil sheet. A distinctive feature of the VE design proposed in this work is the complete elimination of insulating laminating substrates. The free inter-fiber space in such a self-supported architecture begins to function as a microreactor. Under cascade analysis conditions, this creates ideal prerequisites for the local concentration of reaction intermediates directly near the electrocatalytic centers, minimizing the dissipation of intermediates into the bulk solution.

However, the move away from traditional laminating substrates was complicated by the fact that the macroporous nature of carbon veil induces a strong capillary effect, causing the supporting electrolyte to inevitably rise through the inter-fiber space from the working zone to the current collector. To address this problem, the fiber in the area separating the working part and current collector was impregnated with cyanoacrylate glue, which prevents the occurrence of the capillary effect [28]. Polymerized cyanoacrylate acts not only as a mechanical sealant but also forms a strict dielectric barrier, which completely blocks the capillary rise of the liquid and prevents an uncontrolled increase in the electroactive area during measurements, ensuring high reproducibility of the VE geometric parameters. This approach resulted in the preservation of the open 3D structure of carbon veil from all sides, which allowed for a high density of modifiers, including the enzyme, and the creation of ideal conditions for substrate diffusion [33].

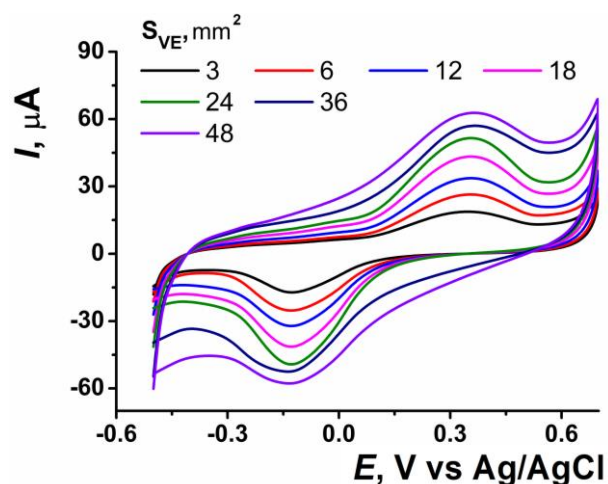


Figure 2 Cyclic voltammograms of unmodified VEs with different S_{VE} values in an equimolar solution (1.0 mM) of $[\text{Fe}(\text{CN})_6]^{3-/4-}$ in a HEPES buffer solution (0.1 M NaNO_3 , pH 7.0) at a scan rate of 0.1 V/s.

To achieve the maximum analytical signal and ensure an optimal signal-to-noise ratio, the dependence of the electrochemical response on the geometric area of the carbon veil electrode (S_{VE}) was investigated in detail. The efficiency of redox reactions occurring at the electrode was evaluated using cyclic voltammetry on unmodified VE in the presence of a standard redox marker - an equimolar (1.0 mM) solution of $\text{K}_3[\text{Fe}(\text{CN})_6]/\text{K}_4[\text{Fe}(\text{CN})_6]$ in a HEPES buffer solution with 0.1 M NaNO_3 , pH 7.0.

The obtained cyclic voltammograms (Fig. 2) demonstrate that an increase in S_{VE} in the range from 3 to 48 mm^2 naturally leads to a general growth in the recorded currents. Analysis of the dependence of I_{pa} on S_{VE} (Fig. S2) revealed strict linearity in the interval from 3 to 24 mm^2 . Within this size range, the macroporous structure operates in an optimal hydrodynamic regime, ensuring uniform diffusion of the redox marker to the fiber surface. The electrochemical process was evaluated using the Randles-Sevcik framework, which describes the relationship between the peak current and the scan rate of the potential. In this context, a linear correlation between the peak current and the square root of the scan rate indicates that the reaction rate is limited by the mass transfer of the redox species from the bulk solution to the electrode surface through diffusion. This confirmation is critical for characterizing the 3D macroporous architecture of the carbon veil, as it demonstrates that the entire effective surface area is accessible for uniform substrate diffusion without significant kinetic or steric hindrances. However, with a further increase in the electrode area (up to 36 and 48 mm^2), a deviation from linearity is observed: the dependence reaches a plateau followed by a decline in absolute I_{pa} values. This effect is directly attributed to the macroporous nature of the carbon material used: at large geometric areas, a sharp, avalanche-like increase in the double-layer charging currents occurs. The significant growth of the background capacitive current severely distorts the shape of the recorded voltammogram, shifting the baseline and reducing the proportion of

pure Faradaic current in the overall recorded response, which leads to a deterioration of the signal-to-noise (S/N) ratio.

Based on the obtained data, an S_{VE} of 24 mm^2 was determined to be optimal for sensor construction, as it allows for the maximum analytical response (I_{pa}) while maintaining an acceptable level of background capacitive currents.

3.2. Formation of the AgNPs/P[5]A nanocomposite on the VE surface

The next stage of sensor development was the formation of a catalytically active layer based on AgNPs stabilized by the P[5]A macrocycle. The choice of this system is due to the ability of redox-active compounds to coordinate silver ions and promote their reduction to the metallic form [29] directly on the carbon fibers. The high electron density of the aromatic fragments of P[5]A not only ensures the uniform distribution of AgNPs during their synthesis but also promotes the local accumulation of the analyte through host-guest supramolecular recognition mechanisms.

In this case, nanoparticle formation proceeds through a spontaneous reduction mechanism: the redox-active hydroquinone fragments of P[5]A act as a mild reducing agent for silver ions. During the synthesis process, Ag^+ ions are coordinated near the macrocycle cavity, followed by electron transfer that results in the formation of metallic silver nuclei (Scheme 1). The formation of metallic silver is driven by the presence of hydroquinone fragments within the P[5]A structure. By analogy with other phenolic macrocycles (such as calixarenes), these units can function as mild reducing agents for Ag^+ ions. This reduction process is further supported by the experimental conditions: the use of a neutral HEPES buffer (pH 7.0) favors the stability of metallic nanoparticles, whereas silver oxide formation typically requires highly alkaline media. Meanwhile, P[5]A serves as a stabilizer, preventing the aggregation of the formed AgNPs and ensuring their uniform distribution across the surface of the carbon fibers.

The surface morphology of the resulting electrode materials was investigated using SEM. The micrograph of the unmodified VE (Fig. 3a) clearly reveals an open 3D macroporous network formed by the chaotic interweaving of smooth cylindrical carbon fibers. Following the application of the AgNPs/P[5]A dispersion, the surface morphology of the fibers changes significantly (Fig. 3b). A uniform distribution of granular structures is observed on the carbon filaments, confirming the successful formation of the nanocomposite coating.

Although the complex 3D topography of the carbon veil precluded a precise calculation of the nanoparticle size distribution from SEM images, the observed granular nanostructures are consistent with recent studies on similar silver-modified electrochemical platforms [34, 35]. This nanoscale morphology is essential for providing the high specific surface area required for efficient electrocatalysis.



Scheme 1 Reaction of AgNPs formation involving P[5]A.

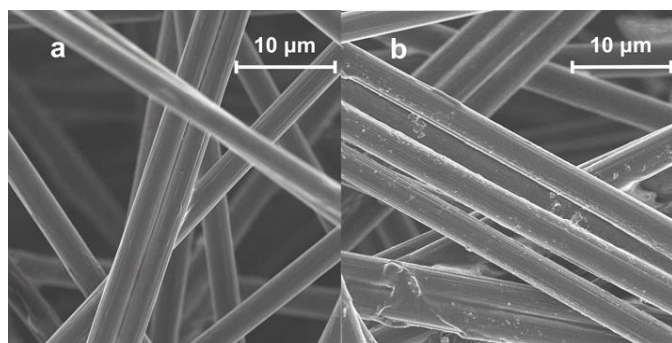


Figure 3 SEM images of the surface morphology: (a) unmodified VE; (b) AgNPs/P[5]A/VE.

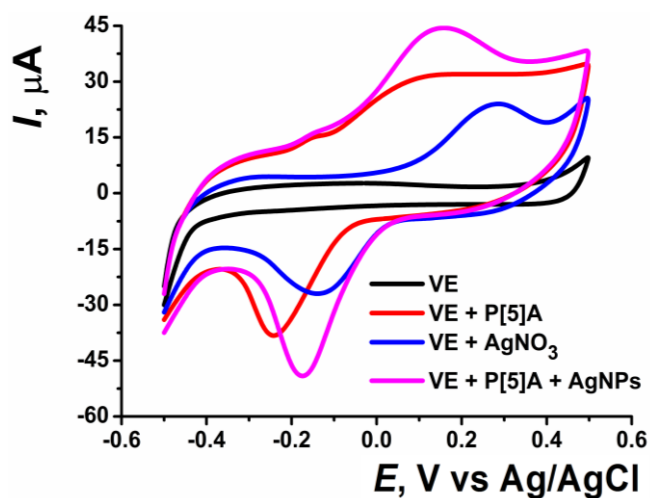


Figure 4 Cyclic voltammograms (second cycle) recorded at VE, P[5]A/VE, AgNO₃/VE, and AgNPs/P[5]A/VE in a HEPES buffer solution (0.1 M NaNO₃, pH 7.0) at a scan rate of 0.1 V/s.

It is important to note that the modification process via drop-casting does not lead to material aggregation in the inter-fiber space or clogging of the macropores. The open carbon veil architecture is fully preserved, which is a critical factor for ensuring unimpeded analyte diffusion into the depth of the electrode and for providing an extensive surface for subsequent efficient enzyme immobilization.

The electrochemical behavior of the obtained modified coatings was studied using cyclic voltammetry (Fig. 4). On the voltammogram recorded for the unmodified VE (black curve), only insignificant background currents are observed. This indicates the absence of electroactive impurities in the starting material. Upon modification of the electrode with pure P[5]A (red curve), the intrinsic electrochemical activity of the macrocycle is manifested: a poorly defined pre-peak (around -0.1 V) followed by a broad oxidation wave is observed in the anodic region. This behavior is characteristic of the stepwise oxidation mechanism of the macrocyclic ring fragments - initially two, and at higher potentials, the three remaining hydroquinone fragments [36].

The control VE modified with AgNO₃ without the macrocycle (blue curve) demonstrates a standard reversible re-

dox pair with an anodic maximum at +0.25 V, corresponding to silver oxidation. However, in the presence of P[5]A (pink curve), the pattern changes drastically, showing a pronounced synergistic effect: the analytical silver oxidation peak shifts toward lower potentials (to +0.05 V), indicating a significant electrocatalytic effect. P[5]A likely acts as a specific ligand that stabilizes silver oxidation products in the reaction zone, thereby reducing the activation energy of the electron transfer process. Concurrently the Faradaic component of the oxidation current increases nearly two-fold compared to the system without the macrocycle. This may be due to P[5]A acting as an electron transfer mediator, improving electron transfer conditions at the system boundaries. Furthermore, due to its preorganization ability [37], the macrocycle promotes the formation of a more developed electroactive surface and prevents nanoparticle aggregation.

3.3. Enzyme sensor for lactose determination

In the next stage of the study, an enzyme sensor for lactose determination was developed based on the modified AgNPs/P[5]A/VE. The operating principle of the biosensor is based on a dual-cascade mechanism: lactose is hydrolyzed by the enzyme, and the released glucose is instantly oxidized at the silver catalytic centers [38]. While the direct non-enzymatic electrooxidation of carbohydrates at metallic centers is well-known [39], such systems often lack the selectivity required for complex food matrices. Our hybrid design combines the superior catalytic activity of AgNPs with the high specificity of lactase, effectively overcoming the typical cross-reactivity issues of purely non-enzymatic sensors when analyzing real dairy products.

Traditionally, rigid chemical cross-linking methods (e.g., EDC/NHS) are used for protein immobilization, which can lead to the loss of the enzyme's native conformation. In this case, however, the non-covalent integration of lactase into the AgNPs/P[5]A/VE composite provided response stability fully comparable to the results of covalent attachment. Such effective protein retention was made possible by the unique microenvironment: the high surface area of the veil and the "stickiness" of AgNPs toward the protein's amino groups, combined with the non-covalent intermolecular bonds of P[5]A, ensure the reliable immobilization of lactase without the loss of its catalytic activity.

The electrochemical response of the developed enzyme sensor upon the addition of various lactose concentrations was recorded using differential pulse voltammetry. On the voltammograms (Fig. 5), a distinct peak is observed at +0.05 V, corresponding to the catalytic oxidation of hydrolysis products on the AgNPs. The increase in this peak magnitude (ΔI) was taken as the analytical signal following lactose addition. Notably, the stepwise oxidation of P[5]A itself appears as a small shoulder in the negative region (around -0.1 V). This signal remains stable and does not overlap with the main analytical peak; consequently, it can serve as an indicator of the nanocomposite layer's integrity.

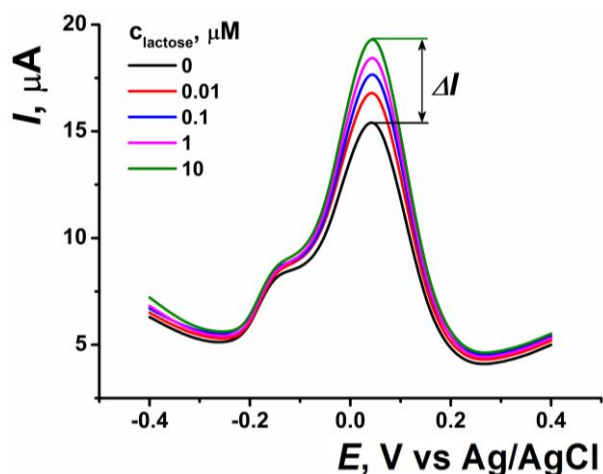


Figure 5 Differential pulse voltammograms (DPVs) recorded at the lactase/AgNPs/P[5]A/VE in a HEPES buffer solution (0.1 M NaNO₃, pH 7.0) in the presence of various lactose concentrations. Potential step: 0.004 V; amplitude: 0.05 V; pulse width: 0.06 s; pulse interval: 0.5 s.

To optimize the biosensor performance, the dependence of the analytical signal on the amount of immobilized enzyme was studied in the range of 0.1 to 4 units (Fig. S3). A nearly linear increase in the analytical signal was observed in the interval up to 2 units, as the process rate is limited by the kinetics of the enzymatic reaction. With a further increase in the enzyme amount, the curve reaches a plateau. At enzyme excess, the response rate becomes limited by either mass transfer (diffusion of lactose molecules from the bulk solution to the electrode surface) or the exhaustion of the electrocatalytic capacity of the AgNPs themselves.

Additionally, a further increase in the amount of high-molecular-weight protein inevitably leads to a thickening of the non-conductive organic layer, which increases steric hindrance and the ohmic resistance of the composite, hindering further current growth. Based on these results, a value of 2 units was selected as the working amount, providing the maximum response while simultaneously avoiding enzyme waste and passivation of the electrode's electroactive surface.

3.4. Determination of lactose in real samples

To evaluate the applicability of the developed biosensor, cows' milk and fermented dairy product samples were analyzed using differential pulse voltammetry. The calibration curve for lactose analysis (Fig. S4) was constructed using matrix-matched calibration for one of the prepared milk samples.

To minimize the passivation of the working electrode surface by sample macro-components, sample preparation was performed, involving the precipitation of protein fractions followed by centrifugation and dilution of the supernatant with the supporting electrolyte. Constructing the calibration curve directly within the prepared diluted matrix allowed for the native accounting of competitive adsorption effects from residual interferents and ensured the correct linearization of the response.

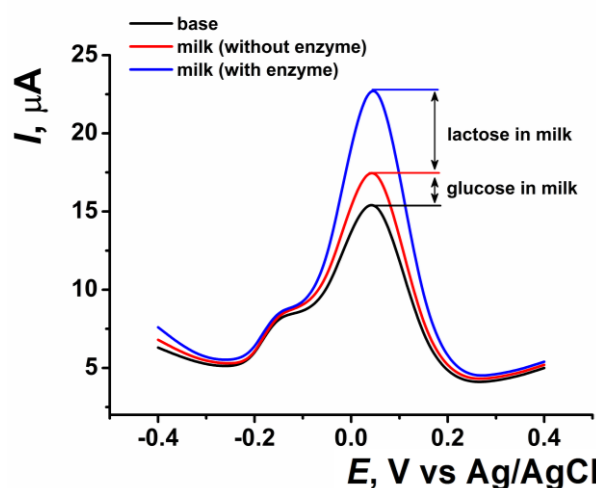


Figure 6 Differential pulse voltammograms recorded at the AgNPs/P[5]A/VE in the absence and presence of lactase in a HEPES buffer solution with added milk (0.1 M NaNO₃, pH 7.0). Potential step: 0.004 V; amplitude: 0.05 V; pulse width: 0.06 s; pulse interval: 0.5 s.

To ensure high accuracy and selectivity of the analysis, a sequential measurement strategy (Fig. 6) was employed: first, the oxidation signal of free endogenous glucose present in the sample was recorded using an enzyme-free AgNPs/P[5]A/VE electrode. Subsequently, measurements were carried out using the enzymatic sensor, recording the total current, which significantly increased due to the catalytic hydrolysis of lactose and the release of additional glucose molecules. The difference between these signals allowed for the accurate calculation of the lactose content, effectively excluding the contribution of background glucose.

The resulting calibration plot for lactose determination using the developed biosensor demonstrates strict linearity in semi-logarithmic coordinates across a wide range from 1×10^{-8} to 2×10^{-4} M ($\Delta I, \mu A = (9.39 \pm 0.06) + (1.05 \pm 0.01) \times \log(C, M)$, $R^2 = 0.9991$) with a limit of detection (LOD) of 3.2 nM (S/N = 3). The pronounced logarithmic nature of the dependence, which is maintained over more than four orders of magnitude, indicates that the rate-limiting step of the electrocatalytic process is not the enzymatic kinetics (Michaelis–Menten), but rather the adsorption of electroactive intermediates on the heterogeneous sensor surface. This behavior is described by the Temkin adsorption isotherm, which assumes the energetic inhomogeneity of the composite's active sites [40].

Due to the macroporous structure of the carbon veil and the presence of the bulky hydrophobic cavities of P[5]A, analyte binding occurs with a competitive displacement effect. The film of supramolecular polymer formed by macrocycle molecules acts as a "buffer" preventing the rapid kinetic saturation of the silver catalytic centers. Maintaining sensitivity up to 2×10^{-4} M of lactose in a concentrated matrix confirms the effectiveness of the chosen cascade mechanism and the synergistic interaction between all components of the modifying layer.

Table 1 Comparison of the electrochemical characteristics of the sensors developed with other electrochemical sensors for lactose determination described in literature.

Sensor	Concentration range, M	LOD, M	Ref.
3-Amine-N-[3-(N-pyrrole)propyl]imidazole bromide/cellobiose dehydrogenase/GCE	5.0×10^{-5} – 3.0×10^{-3}	5.8×10^{-7}	[41]
Lactase/Glutaraldehyde cross-linked/Gold disc electrode	1.0×10^{-5} – 3.5×10^{-4}	1.4×10^{-6}	[42]
Graphitic carbon nitride/magnetic chitosan composite/cellobiose dehydrogenase/GCE	9.0×10^{-4} – 1.0×10^{-1}	3.0×10^{-4}	[43]
Polypyrrole-based imprinted polymer/Gold electrode	1.0×10^{-5} – 1.2×10^{-4}	4.16×10^{-5}	[44]
Gold nanoparticles/MnO ₂ /g-C ₃ N ₄ decorated TiO ₂ /Indium tin oxide	8.0×10^{-6} – 2.5×10^{-3}	2.3×10^{-7}	[45]
Electropolymerized pyrrole molecularly imprinted polymer /graphite paper electrode	1.0×10^{-9} – 1.0×10^{-6}	8.8×10^{-10}	[46]
Lactase/3-mercaptopropionic acid/self-assembled monolayer modified gold	1.5×10^{-6} – 1.2×10^{-4}	4.6×10^{-7}	[47]
Lactase/AgNPs/P[5]A/VE	1.0×10^{-8} – 2.0×10^{-4}	3.2×10^{-9}	This work

Table 2 Determination of lactose in real dairy products using the developed biosensor and the HPLC reference method (n = 5).

Sample	Independent laboratory analysis (HPLC), mM	Lactase/ AgNPs/ P[5]A/VE, mM
Milk	158 ± 5	162 ± 7
Lactose-free milk	< 0.5	0.32 ± 0.05
Yogurt	84 ± 3	86 ± 4
Lactose-free yogurt	< 0.5	0.15 ± 0.03

Comparison of the analytical performance of the developed biosensor with existing analogs (Table 1) confirms the high efficiency of the proposed approach. Most systems described in the literature exhibit detection limits in the micromolar or sub-millimolar range. Against this backdrop, the lactase/AgNPs/P[5]A/VE sensor developed in this work demonstrates outstanding sensitivity with a detection limit of 3.2 nM.

The only sensor in the table that slightly outperforms it in this metric is based on a molecularly imprinted polymer on a graphite paper electrode (LOD = 0.88 nM). It is worth noting that this sensor shares certain structural similarities with our platform, as both utilize a flexible carbon material as a matrix. However, it is important to emphasize that molecular imprinting technology is a multi-stage and expensive process: it requires the precise optimization of electropolymerization conditions followed by the thorough removal of template molecules using toxic solvents. Incomplete template removal or damage to the polymer matrix

during the cleaning step often leads to poor signal reproducibility. Thus, our proposed method for assembling the nanocomposite biosensor achieves performance comparable to its analogs while maintaining simplicity, cost-effectiveness, and high operational flexibility, all while adhering to the principles of “green chemistry”.

To evaluate the reliability and analytical validity of the developed biosensor, a screening of commercial dairy products with various labeled lactose contents was performed. The direct calculation of the signals for the prepared milk and yogurt samples, using the matrix-matched calibration equation for each sample (considering the dilution factor), allowed us to determine the actual lactose concentrations (Table 2).

These results were compared with independent analysis data obtained via high-performance liquid chromatography (HPLC) as a reference method. As shown by the data, the results obtained using the nanocomposite biosensor demonstrate a high degree of correlation with the reference method for standard milk and yogurt samples. The lower lactose concentration in yogurt compared to whole milk naturally reflects the process of bacterial fermentation of carbohydrates.

The analysis of specialized lactose-free products deserves particular attention. While the standard laboratory method proved insufficiently sensitive for the accurate quantification of trace amounts of lactose (yielding values below the limit of quantification (LOQ)), the proposed electrochemical biosensor, due to its ultra-low limit of detection, allowed for the highly accurate measurement of residual lactose at levels of 0.15–0.32 mM.

The operational stability of the biosensor was verified by 50 consecutive differential-pulse voltammetry measurements in the presence of lactose (Fig. S5). The results demonstrated high signal stability (retention 96%), while the constant redox response of the P[5]A macrocycle confirmed the structural integrity of the nanocomposite layer. The batch-to-batch reproducibility of the proposed biosensor was evaluated by testing 10 independent electrodes fabricated on different days. The relative standard deviation (RSD) of their amperometric responses was 4.4%. Furthermore, the long-term storage stability was assessed: after 90 days of storage at 4 °C, the sensor retained 91% of its initial analytical response, confirming the efficiency of the non-covalent enzyme immobilization.

This opens broad prospects for applying the developed sensor platform to the strict quality control of dietary and hypoallergenic food products. The results confirm the high efficiency of the proposed biosensor design using biosimilar supramolecular systems and the selected sample preparation methodology for the selective electroanalysis of complex food matrices.

4. Limitations

The study has several limitations: the susceptibility of the nanostructured surface to biofouling by dairy proteins and lipids necessitates a mandatory pre-treatment stage, complicating "in-field" application; the presence of endogenous sugars in real samples precludes a single-stage measurement, requiring a differential strategy with paired sensors; the manual drop-casting method used for electrode modification results in batch-to-batch variability. These gaps highlight the need for future work on automated sensor fabrication, surface anti-fouling strategies, and the development of integrated portable devices for rapid on-site analysis.

Conclusions

In this study, a novel architecture for a stand-alone electrochemical sensor based on carbon veil was successfully designed and implemented. A key engineering milestone was the development of a self-supported carbon veil electrode, in which a cyanoacrylate barrier effectively isolated the working zone from the current collector without disrupting the integrity of the microporous 3D fiber network. Optimization of the platform's geometric parameters resulted in a high signal-to-noise (S/N) ratio, providing a robust foundation for the development of an ultrasensitive biosensor.

The formation of the AgNPs/pillar[5]arene nanocomposite on the fiber surface provided an efficient catalytic environment for detecting enzymatic hydrolysis products. It was demonstrated that pillar[5]arene not only stabilizes the silver nanoparticles but also actively participates in the electron transfer process, promoting analyte pre-organization in the reaction zone through supramolecular recognition mechanisms. The application of "mild" non-covalent lactase immobilization allowed for the integration of the biorecognition element without the loss of its native activity, as evidenced by the stability of the analytical response over a series of measurements.

The developed system demonstrated a limit of detection of 3.2 nM. A comparative analysis with the reference HPLC method showed high convergence of results for the determination of lactose in milk and yogurt. Of particular significance is the biosensor's ability to quantify trace amounts of lactose in "lactose-free" products—levels that remain inaccessible to standard laboratory techniques. This confirms the potential of the proposed platform as a basis for creating portable food quality analyzers.

Supplementary materials

This manuscript contains supplementary materials, which are available on the corresponding online page.

Data availability statement

The raw/processed data required to reproduce the above findings cannot be shared at this time as the data also forms part of an ongoing study.

Acknowledgments

None.

Author contributions

Conceptualization: D.S, I.S.
 Data curation: K.K.
 Formal Analysis: D.S, K.K., E.S.
 Funding acquisition: D.S.
 Investigation: D.S., K.K, E.S., A.R.
 Methodology: D.S., I.S.
 Project administration: D.S., I.S.
 Resources: I.S., A.R.
 Software: E.S., A.R.
 Supervision: I.S.
 Validation: D.K., K.K., A.R.
 Visualization: D.S.
 Writing – original draft: D.K., K.K.
 Writing – review & editing: D.S., E.S., I.S.

Conflict of interest

The authors declare no conflict of interest.

Additional information

Author Scopus IDs:

Kamila Ruslanovna Karaguzina, [59475849100](https://orcid.org/0000-0002-5947-5849);
 Dmitry Ivanovich Stoikov, [57204267835](https://orcid.org/0000-0002-5720-4267);
 Dominika Kappo, [55900821800](https://orcid.org/0000-0002-5590-0821);
 Alexey Mikhailovich Rogov, [6602887534](https://orcid.org/0000-0002-6602-8875).
 Ivan Ivanovich Stoikov, [6602887534](https://orcid.org/0000-0002-6602-8875).

Website:

Kazan (Volga region) Federal University, <https://kpfu.ru/Eng/>.

References

- Karimi-Maleh H, Karimi F, Alizadeh M, Sanati AL. Electrochemical Sensors, a bright Future in the fabrication of portable Kits in analytical Systems. *Chem Rec.* 2020; 20(7): 682-692. [doi:10.1002/tcr.201900092](https://doi.org/10.1002/tcr.201900092)
- Ghalkhani M, Bakirhan NK, Ozkan SA. Combination of efficiency with Easiness, Speed, and cheapness in development of sensitive Electrochemical Sensors. *Crit Rev Anal Chem.* 2020; 50(6): 538-553. [doi:10.1080/10408347.2019.1664281](https://doi.org/10.1080/10408347.2019.1664281)
- Baranwal J, Barse B, Gatto G, Broncova G, Kumar A. Electrochemical sensors and their Applications: A Review. *Chemosensors.* 2022; 10(9): 363. [doi:10.3390/chemosensors10090363](https://doi.org/10.3390/chemosensors10090363)
- Mohan JM, Amreen K, Javed A, Dubey SK, Goel S. Emerging trends in miniaturized and microfluidic electrochemical sensing platforms. *Curr Opin Electrochem.* 2022; 33: 100930. [doi:10.1016/j.coelec.2021.100930](https://doi.org/10.1016/j.coelec.2021.100930)
- Wijayanti SD, Tsvik L, Haltrich D. Recent advances in electrochemical Enzyme-based Biosensors for food and beverage Analysis. *Foods.* 2023; 12(18): 3355. [doi:10.3390/foods12183355](https://doi.org/10.3390/foods12183355)
- Pokrzywnicka M, Koncki R. Disaccharides Determination: A review of analytical Methods. *Crit Rev Anal Chem.* 2018; 48(3): 186-213. [doi:10.1080/10408347.2017.1391683](https://doi.org/10.1080/10408347.2017.1391683)
- Dominici S, Marescotti F, Sanmartin C, Macaluso M, Taglieri I, Venturi F, Zinnai A, Facioni MS. Lactose: Characteristics, food and Drug-related Applications, and its Possible substitutions in meeting the needs of people with lactose Intolerance. *Foods.* 2022; 11(10): 1486. [doi:10.3390/foods11101486](https://doi.org/10.3390/foods11101486)
- Silanikove N, Leitner G, Merin U. The interrelationships between lactose Intolerance and the modern Dairy Industry: global Perspectives in evolutionary and historical Backgrounds. *Nutrients.* 2015; 7(9): 7312-7331. [doi:10.3390/nu7095340](https://doi.org/10.3390/nu7095340)

9. Li A, Zheng J, Han X, Yang S, Cheng S, Zhao J, Zhou W, Lu Y. Advances in Low-Lactose/Lactose-free Dairy products and their Production. *Foods*. 2023; 12(13): 2553. [doi:10.3390/foods12132553](https://doi.org/10.3390/foods12132553)
10. Portnoy M, Barbano DM. Lactose: Use, measurement, and expression of results. *J Dairy Sci*. 2021; 104(7): 8314-8325. [doi:10.3168/jds.2020-18706](https://doi.org/10.3168/jds.2020-18706)
11. Zhang Y, Zhang W, Hou J, He J, Li K, Li Y, Xu D. Determination of sugars and sugar alcohols in infant formula by high performance liquid chromatography with evaporative light-scattering detector. *J Chromatogr B*. 2023; 1217: 123621. [doi:10.1016/j.jchromb.2023.123621](https://doi.org/10.1016/j.jchromb.2023.123621)
12. Sarkozy D, Farsang R, Szigeti M, Austin S, Lock S, Guttman A. Capillary electrophoresis analysis of industrial galactooligosaccharides. *J Pharm Biomed Anal*. 2023; 233: 115434. [doi:10.1016/j.jpba.2023.115434](https://doi.org/10.1016/j.jpba.2023.115434)
13. Ribeiro DCSZ, Neto HA, Lima JS, de Assis DCS, Keller KM, Campos SVA, Oliveira DA, Fonseca LM. Determination of the lactose content in low-lactose milk using Fourier-transform infrared spectroscopy (FTIR) and convolutional neural network. *Heliyon*. 2023; 9(1): e12898. [doi:10.1016/j.heliyon.2023.e12898](https://doi.org/10.1016/j.heliyon.2023.e12898)
14. Marx MG. Emerging trends of electrochemical Sensors in food Analysis. *Electrochem*. 2023; 4(1): 42-46. [doi:10.3390/electrochem4010004](https://doi.org/10.3390/electrochem4010004)
15. Yuan Y, Shen J, Salmon S. Developing enzyme Immobilization with fibrous Membranes: longevity and characterization Considerations. *Membranes*. 2023; 13(5): 532. [doi:10.3390/membranes13050532](https://doi.org/10.3390/membranes13050532)
16. Singh RV, Singh B, Kumar A, Sambyal K, Karuppanan KK, Lee JK. Enzyme immobilization on nanomaterials and their Applications. *Materials*. 2025; 18(17): 4106. [doi:10.3390/ma18174106](https://doi.org/10.3390/ma18174106)
17. Stoikov DI, Karaguzina KR, Kappo D, Shurpik DN, Stoikov II, Porfireva AV. Xanthine determination in food samples using a carbon veil-based bi-enzyme amperometric sensor. *Microchim Acta*. 2026; 193(4): 257. [doi:10.1007/s00604-026-08002-w](https://doi.org/10.1007/s00604-026-08002-w)
18. You J, Gajda I, Greenman J, Ieropoulos IA. Integration of Cost-efficient Carbon electrodes into the development of microbial Fuel Cells. *Carbon Mater: Chem Phys*. 2022; 11: 43-57. [doi:10.1007/978-3-030-81827-2_3](https://doi.org/10.1007/978-3-030-81827-2_3)
19. Stoikov DI, Karaguzina KR, Kappo D, Shurpik DN, Stoikov II, Porfireva AV, Evtugyn GA. Electrochemical flow-through sensor based on a carbon veil/sulfanilamide pillar[5]arene derivative composite for determining total antioxidant capacity. *Microchem J*. 2026; 224: 117630. [doi:10.1016/j.microc.2026.117630](https://doi.org/10.1016/j.microc.2026.117630)
20. Hou L, Bi S, Lan B, Zhao H, Zhu L, Xu Y, Lu Y. A novel and ultrasensitive nonenzymatic glucose sensor based on pulsed laser scribed carbon paper decorated with nanoporous nickel network. *Anal Chim Acta*. 2019; 1082: 165-175. [doi:10.1016/j.aca.2019.07.056](https://doi.org/10.1016/j.aca.2019.07.056)
21. Wang T, Reid RC, Minter SD. A paper-based mitochondrial electrochemical biosensor for pesticide detection. *Electroanalysis*. 2016; 28(4): 854-859. [doi:10.1002/elan.201500487](https://doi.org/10.1002/elan.201500487)
22. Torrinha A, Martins M, Tavares M, Delerue-Matos C, Morais S. Carbon paper as a promising sensing material: characterization and electroanalysis of ketoprofen in wastewater and fish. *Talanta*. 2021; 226: 122111. [doi:10.1016/j.talanta.2021.122111](https://doi.org/10.1016/j.talanta.2021.122111)
23. Li S, Kim M, Song YE, Son SH, Kim H, Jae J, Yan Q, Fei Q, Kim JR. Housing of electrosynthetic biofilms using a roll-up carbon veil electrode increases CO₂ conversion and faradaic efficiency in microbial electrosynthesis cells. *Bioresour Technol*. 2024; 393: 130157. [doi:10.1016/j.biortech.2023.130157](https://doi.org/10.1016/j.biortech.2023.130157)
24. Lu W, Hartman R, Qu L, Dai L, Kulkarni K, Carnahan D. Combining nanostructured carbon electrodes and ionic liquid electrolytes to develop new electrochemical capacitors. *ECS Trans*. 2008; 16(1): 69-75. [doi:10.1149/1.2985628](https://doi.org/10.1149/1.2985628)
25. Bukharinova MA, Stozhko NY, Novakovskaya EA, Khamzina EI, Tarasov AV, Sokolov SV. Developing activated carbon veil electrode for sensing salivary uric acid. *Biosensors*. 2021; 11(8): 287. [doi:10.3390/bios11080287](https://doi.org/10.3390/bios11080287)
26. Bukharinova MA, Khamzina EI, Kolotygina VY, Stozhko NY. A voltammetric sensor based on carbon veil modified with graphene and phytosynthesized cobalt oxide nanoparticles for the determination of food dyes tartrazine (E102) and allura red (E129). *J Anal Chem*. 2023; 78(12): 1679-1687. [doi:10.1134/S106193482312002X](https://doi.org/10.1134/S106193482312002X)
27. Brainina KZ, Bukharinova MA, Stozhko NY, Sokolov SV, Tarasov AV, Vidrevich MB. Electrochemical sensor Based on a carbon Veil modified by phytosynthesized Gold nanoparticles for determination of ascorbic Acid. *Sensors*. 2020; 20(6): 1800. [doi:10.3390/s20061800](https://doi.org/10.3390/s20061800)
28. Kang H, Bui TH, Han W, Lee YI, Shin JH. A novel low-cost and simple fabrication technique for a paper-based analytical device using super glue. *Anal Chim Acta*. 2024; 1329: 343174. [doi:10.1016/j.aca.2024.343174](https://doi.org/10.1016/j.aca.2024.343174)
29. Kuzin Y, Porfireva A, Stepanova V, Evtugyn V, Stoikov I, Evtugyn G, Hianik T. Impedimetric detection of DNA damage with the sensor Based on silver Nanoparticles and neutral Red. *Electroanalysis*. 2015; 27(12): 2800-2808. [doi:10.1002/elan.201500312](https://doi.org/10.1002/elan.201500312)
30. Wei M, Qiao Y, Zhao H, Liang J, Li T, Luo Y, Lu S, Shi X, Lu W, Sun X. Electrochemical non-enzymatic glucose sensors: recent progress and perspectives. *Chem Commun*. 2020; 56(93): 14553-14569. [doi:10.1039/DoCC05650B](https://doi.org/10.1039/DoCC05650B)
31. Ogoshi T, Kanai S, Fujinami S, Yamagishi T, Nakamoto Y. para-bridged Symmetrical Pillar[5]arenes: their Lewis acid Catalyzed synthesis and Host-guest Property. *J Am Chem Soc*. 2008; 130(15): 5022-5023. [doi:10.1021/ja711260m](https://doi.org/10.1021/ja711260m)
32. GOST 34304-2017 Moloko i molochnye produkty. Metod opredeleniya laktozy i galaktozy [State Standard GOST 34304-2017. Milk and dairy products. Method for determination of lactose and galactose]. Moscow: Standartinform; 2018. 14 p. Russian.
33. P. Theodosiou, J. Greenman, I.A. Ieropoulos / Developing 3D-printable Cathode electrode for monolithically Printed microbial Fuel cells (MFCs) // *Molecules*. - 2020. - V. 25(16). - P. 3635
34. Saqib M, Dorozhko EV, Berek J, Korotkova EI, Semin VO, Kolobova E, Erkovich AV. Sensitive electrochemical sensing of carbosulfan in food products on laser reduced graphene oxide sensor decorated with silver nanoparticles. *Microchem J*. 2024; 207: 112253. [doi:10.1016/j.microc.2024.112253](https://doi.org/10.1016/j.microc.2024.112253)
35. Dorozhko E, Kazachinskaya E, Kononova Y, Zaikovskaya A, Berek J, Korotkova E, Kolobova E, Sheveleva P, Saqib M. Electrochemical immunoassay of antibodies using freshly prepared and aged conjugates of silver nanoparticles. *Talanta*. 2023; 253: 124028. [doi:10.1016/j.talanta.2022.124028](https://doi.org/10.1016/j.talanta.2022.124028)
36. Smolko VA, Shurpik DN, Shamagsumova RV, Porfireva AV, Evtugyn VG, Yakimova LS, Stoikov II, Evtugyn GA. Electrochemical behavior of pillar[5]arene on glassy carbon electrode and its interaction with Cu²⁺ and Ag⁺ ions. *Electrochim Acta*. 2014;147:726-734. [doi:10.1016/j.electacta.2014.10.007](https://doi.org/10.1016/j.electacta.2014.10.007)
37. Stoikov DI, Porfir'eva AV, Shurpik DN, Stoikov II, Evtugyn GA. Electrochemical DNA sensors on the basis of electropolymerized thionine and azure B with addition of pillar[5]arene as an electron transfer mediator. *Russ Chem Bull*. 2019; 68(2): 431-437. [doi:10.1007/s1172-019-2404-8](https://doi.org/10.1007/s1172-019-2404-8)
38. Quan H, Park SU, Park J. Electrochemical oxidation of glucose on silver nanoparticle-modified composite electrodes. *Electrochimica Acta*. 2010; 55(7): 2232-2237. [doi:10.1016/j.electacta.2009.11.074](https://doi.org/10.1016/j.electacta.2009.11.074)
39. Wei M, Qiao Y, Zhao H, Liang J, Li T, Luo Y, Lu S, Shi X, Lu W, Sun X. Electrochemical non-enzymatic glucose sensors: recent progress and perspectives. *Chem Commun*. 2020; 56(93): 14553-14569. [doi:10.1039/DoCC05650B](https://doi.org/10.1039/DoCC05650B)
40. Tovbin YuK. Razvitie idei M.I. Temkina v fizicheskoi khimii [Development of M.I. Temkin's Ideas in Physical Chemistry]. *Kinet. Katal*. 2019;60(4):428-39. Russian. [doi:10.1134/S045388119040221](https://doi.org/10.1134/S045388119040221)

41. Wu H. Electrochemical sensor based on ionic liquid for detection of lactose content in dairy products. *J Food Meas Charact.* 2024; 18(1): 313-319. [doi:10.1007/s11694-023-02181-3](https://doi.org/10.1007/s11694-023-02181-3)
42. Sánchez-Salcedo R, Geddes DT, Voelcker NH. A Single-enzyme Electrochemical biosensor for lactose Detection in human Breastmilk and dairy Products. *ACS Meas Sci Au.* 2026. [doi:10.1021/acsmesuresciau.5c00207](https://doi.org/10.1021/acsmesuresciau.5c00207)
43. Nasiri H, Baghban H, Teimuri-Mofrad R, Mokhtarzadeh A. Graphitic carbon nitride/magnetic chitosan composite for rapid electrochemical detection of lactose. *Int Dairy J.* 2023; 136: 105489. [doi:10.1016/j.idairyj.2022.105489](https://doi.org/10.1016/j.idairyj.2022.105489)
44. Perez-Gonzalez C, Garcia-Hernandez C, Garcia-Cabezon C, Rodriguez-Mendez ML, Martin-Pedrosa F. Advanced characterization in molecularly imprinted polypyrrole for potentiometric lactose sensing. *Microchem J.* 2025; 216: 114709. [doi:10.1016/j.microc.2025.114709](https://doi.org/10.1016/j.microc.2025.114709)
45. Çakıroğlu B, Demirci YC, Gökgöz E, Özacar M. A photoelectrochemical glucose and lactose biosensor consisting of gold nanoparticles, MnO₂ and g-C₃N₄ decorated TiO₂. *Sens Actuators B: Chem.* 2019; 282: 282-289. [doi:10.1016/j.snb.2018.11.064](https://doi.org/10.1016/j.snb.2018.11.064)
46. da Silva JL, Buffon E, Beluomini MA, Pradela-Filho LA, Gouveia Araújo DA, Santos AL, Takeuchi RM, Stradiotto NR. Non-enzymatic lactose molecularly imprinted sensor based on disposable graphite paper electrode. *Anal Chim Acta.* 2021; 1143: 53-64. [doi:10.1016/j.aca.2020.11.030](https://doi.org/10.1016/j.aca.2020.11.030)
47. Dortez S, Crevillen AG, Escarpa A, Cinti S. Electroanalytical paper-based device for reliable detection and quantification of sugars in milk. *Sens Actuators B: Chem.* 2024; 398: 134704. [doi:10.1016/j.snb.2023.134704](https://doi.org/10.1016/j.snb.2023.134704)